Colloid Polym Sci (2005) 283: 1226–1232
DOI 10.1007/s00396-005-1302-9

SHORT COMMUNICATION

A. Khanal
K. Nakashima
N. Kawasaki
Y. Oishi
M. Uehara
H. Nakamura
Y. Tajima

Fabrication of organic–inorganic nano-complexes using ABC type triblock copolymer and polyoxotungstates

Received: 12 October 2004
Accepted: 24 December 2004
Published online: 11 May 2005

A. Khanal · K. Nakashima (✉)
N. Kawasaki · Y. Oishi
Department of Chemistry, Faculty of Science and Engineering, Saga University, Honjo, Saga, Saga 840-8502, Japan
E-mail: nakashik@cc.saga-u.ac.jp
Tel.: +81-952-288850
Fax: +81-952-288548

M. Uehara · H. Nakamura
Micro-chemical Processing Group, National Institute of Advanced Industrial Science and Technology, Tosu Saga 841-0052, Japan

Y. Tajima
Infection Control Sciences, Postgraduate School of Medicine, Juntendo University, Hongo, Bunkyo-ku, Tokyo 113-8421, Japan

Abstract New organic–inorganic nano-complexes were produced from a micelle of tri-block polymers; poly(styrene)-*b*-poly(2-vinylpyridine)- *b*-poly (ethylene oxide) (PS-PVP-PEO) and tungsten compounds such as tungstate (W_1^{2-}), undecatungstophospate (PW_{11}^{7-}) and undecatungstosilicate (SiW_{11}^{8-}) in acidic aqueous solutions. The size and morphology of the complexes were characterized by measurements of dynamic light scattering, atomic force microscopy, and scanning electron microscopy. This complex is assembled mainly by the charge interaction between the inorganic polyanions and the positively charged PVP block in the PS-PVP-PEO molecule, which was confirmed by zeta-potential and fluorescence spectroscopic studies. In the absence of the inorganic anions, the zeta-potential of the micelle was +11 mV at pH 3 due to the positive charge of the PVP block. When the inorganic anion was mixed with the PS-PVP-PEO micelle, decrease in the zeta-potential due to charge neutralization occurred with incorporation of inorganic anions into the PS-PVP-PEO micelle. The minimum zeta-potential was 0, −33, and −35 mV for W_1^{2-} / PS-PVP-PEO, PW_{11}^{7-} /PS-PVP-PEO, and SiW_{11}^{8-} /PS-PVP-PEO complexes, respectively. Excess negative charge which occurred in the latter two complexes indicates that PS-PVP-PEO molecules bound PW_{11}^{7-} and SiW_{11}^{8-} by forces other than charge interaction. In addition, the incorporation of an inorganic polyanion into the micelle gave a new morphology to the micelle. In the absence of the polyanion, the PS-PVP-PEO micelles showed an extended conformation due to repulsive forces working among the positively charged PVP blocks. Addition of the polyanion caused the formation of shrunken forms of the micelles, since the charge repulsion was cancelled by the polyanion. This feature may be useful in developing a new type of functioning micelle.

Keywords Polyoxotungstate · Undecatungstophospate · Undecatungstosilicate · Tungstate · Poly(styrene)-*b*-poly(2-vinylpyridine)-*b*-poly(ethylene oxide)

Abbreviations

PW_{11}^{7-}	Undecatungstophosphate, $(PW_{11}O_{39})^{7-}$
SiW_{11}^{8-}	Undecatungstosilicate, $(SiW_{11}O_{39})^{8-}$
W_1^{2-}	Tungstate (WO_4^{2-})
POT(s)	Polyoxotungstate(s)
PS-PVP-PEO	Poly(styrene)-*b*-poly (2-vinylpyridine)-*b*-poly(ethylene oxide)
ADN	Apparent degree of neutralization
DLS	Dynamic light scattering
AFM	Atomic force microscopy
SEM	Scanning electron microscopy
EPM	Electrophoretic mobility
Py	Pyrene

Introduction

The synthesis of chemically and physically well-defined nano-particles is of great interest to various fields of science: e.g., applications of nano-sized materials have been eagerly investigated in pharmacology, bioengineering, medical chemistry, and industries such as ceramics. Making a polymeric micelle is one of the most promising fields in nano-technologies, and several different methodologies using chelating agents [1–4], ionic substances [5, 6], or surfactant [7–12] have been developed to control the size and morphology of nano-particles over the past few decades.

Nowadays, various hybrid micelles composed of organic and inorganic materials are fabricated, breaking fresh ground in nano-science [13–18]. However, only a quite few products using ABC type triblock copolymers have been worked on till date [19, 20]. Recently, Jèrôme et al. reported that a gold salt was incorporated into chemically well-defined "core-shell-corona"-type micelles which were made by poly(styrene)-*b*-poly(2-vinylpyridine)-*b*-poly(ethylene oxide) (PS-PVP-PEO) triblock copolymers in aqueous solution [19, 20]. Structurally, these micelles have a "frozen" *PS core*, a positively charged *PVP shell* as an intermediate layer, and an outer *PEO corona* under acidic conditions [19–23]. The whole micelle structure showed an extended conformation at pH $<$ 5 due to the repulsive forces working among positively charged PVP blocks. The addition of some anionic substances into this micelle cancelled the repulsive forces electrically, making the PVP block insoluble in water. This process indued a conformational change of the micelle from an extended form to a shrunken one.

By using this feature of PS-PVP-PEO micelle binding anionic substances, we can fabricate novel organic-inorganic hybrid nano-complexes. In this study, inorganic polyanions such as undecatungstophosphate ($(PW_{11}O_{39})^{7-}$, PW_{11}^{7-}) and undecatungstosilicate ($(SiW_{11}O_{39})^{8-}$, SiW_{11}^{8-}) were used as a counteranion. These two compounds are well known as "Keggin"-structural polyoxotungstates (POTs) displaying many biochemical activities [24] such as being photocatalysts, antiviral agents [25, 26], and anticoagulants [27, 28]. Recently, it was found that POTs have a strong sensitizing effect on methicillin-resistant *Staphylococcus aureus* in β-lactam antibiotics [24, 29–32]. Therefore, some new functioning micelles can be formed from such bioactive material by using molecular hybrid techniques. The nano-complexes thus prepared were characterized by measurements of zeta-potential, dynamic light scattering (DLS), atomic force microscopy (AFM), and scanning electron microscopy (SEM).

Experimental

Materials

PS-PVP-PEO was purchased from Polymer Source Inc. (Dorval, Canada), and used without further purification. The number-averaged molecular weights of PS, PVP, and PEO block are 14,100, 12,300, and 35,000, respectively. Sodium tungstate (Na_2WO_4, W_1^{2-}), dodecatungstophosphoric acid ($H_3(PW_{12}O_{40})$, PW_{12}) and dodecatungstosilicic acid ($H_4(SiW_{12}O_{40})$, SiW_{12}) were obtained from Wako Pure Chemicals (Osaka, Japan). Highly purified water by Millipore MiliQ system was used throughout the experiments. PW_{11}^{7-} and SiW_{11}^{8-} were prepared by partial hydrolysis of PW_{12} and SiW_{12}, and were purified by recrystalization prior to the experiments [29–33].

Preparation of organic–inorganic nano-complexes

After PS-PVP-PEO was dissolved in 0.01 M HCl, the mixture was heated at 65 °C for 2 h. The solution was cooled and the concentration was adjusted to 0.1 g/L with water. The solution was slowly stirred for several days until it turned clear (stock solution, pH = ~2). Solutions to make micelles were prepared by diluting the stock solution with water, and the pH was adjusted to a desired level by adding 0.1 M NaOH, where needed.

Upon adding tungsten compounds to the PS-PVP-PEO micelles, it is convenient to express the amount of added compound on a charge basis. Thus, a parameter called the *apparent degree of neutralization* (ADN) was tentatively defined by the following formula:

$$\mathrm{ADN} = \frac{\text{Normality of tungsten compounds}}{\text{Normality of pyridine unit}} \times 100. \quad (1)$$

The numerator was calculated by (molarity of added anionic compound) × (anionic valence): e.g., 1 mM PW_{11}^{7-} is expressed as (1×7 =) 7 mN. The denominator was estimated from the pyridine content in PS-PVP-PEO micelles.

All the solutions used in the experiments, i.e., tungsten compounds and PS-PVP-PEO micelles, were stable and transparent under the experimental conditions for several weeks.

Zeta-potential measurements

Electrophoretic mobility (EPM) of the test sample was measured at 25 °C with ELS-8000 (Otsuka, Tokyo, Japan). The zeta-potential of the sample was calculated from the EPM using the Smoluchowski's equation:

$$\mu_E = \frac{\zeta\varepsilon}{\eta},$$

where μ_E is EPM, ζ the zeta-potential, ϵ the permittivity of solvent, and η the viscosity of solvent.

Dynamic light scattering measurements

Dynamic light scattering was measured with ELS-800 (Otsuka, Tokyo, Japan) at a fixed 90 ° scattering angle. Correlation functions were analyzed by a histogram method and used to determine the diffusion coefficient (D) of the nano-complexes in the test sample. Hydrodynamic radius (R_h) was calculated from D by using the Stokes–Einstein's equation:

$$R_h = \frac{k_B T}{6\pi\eta D},$$

where k_B is Boltzmann constant, T the absolute temperature, and η the solvent viscosity.

Atomic force microscopy

Atomic force microscopy images were obtained in dynamic force mode (corresponding to the tapping mode) with SPA 300 unit and SPI 3700 control station (Seiko Instruments Industry, Tokyo, Japan) in the room air. The samples for AFM observations were prepared by evaporating a drop of the test sample on a mica plate freshly cleaved in air.

Scanning electron microscopy

Scanning electron microscopic techniques were carried out with S-5200, Type-SK2 electron microscope (Hitachi High Technologies, Tokyo, Japan). The samples were prepared by evaporating a drop of the test sample solution on the glass plate under vacuum conditions.

Fluorescence spectroscopy

Pyrene (Py) was used as a fluorescent probe. A small portion of a methanol solution of Py was taken into a volumetric flask, and methanol was gradually evaporated by heating under a nitrogen gas stream. Then, the solution of PS-PVP-PEO complexes mixed with tungsten compounds was added, and the final concentration of Py in the test sample was kept constant at 0.6 μM, which is near to its saturation level in water at 22 °C. Steady-state fluorescence spectra of the air-equilibrated samples (in 1×1 cm quartz cell) were recorded with FP-6500 fluorescence spectrophotometer (JASCO, Tokyo, Japan) using right angle geometry. The band widths of the light wavelength were 3 and 1 nm for excitation (334 nm) and emission, respectively.

Results and discussion

Zeta-potential of nano-complexes

Micelles prepared in this report are unique in the following features: (1) This is a molecular hybrid of both organic and inorganic compounds. (2) The micelle structure is maintained by charge interaction in addition to hydrophilic–hydrophobic dynamics. (3) POTs with a high anionic valency (−7∼−8) present in a small molecular diameter (∼10Å) are incorporated in the core part. This may consolidate the structure of the micelle, and therefore, it is important to know how POTs interact with the micelles.

Figure 1 shows the effect of counteranions on the zeta-potential of the nano-complexes. In the absence of the inorganic anions, the zeta-potential of the micelle was +11 mV at pH 3 due to the positive charge of the PVP block in the PS-PVP-PEO micelle. When W_1^{2-} was used as a counteranion (Fig. 1a), the zeta-potential of the micelle was continuously decreased as ADN increased. However, the zeta-potential did not become 0 mV at 100% ADN, and an excess amount of W_1^{2-} (ADN = 220%) was required to cancel the positive charge. This means that: (1) The affinity of W_1^{2-} to the PVP block was relatively weak, and only ∼50% of W_1^{2-} could be bound by the PVP block at most. (2) Steric hindrance occurred, thereby preventing W_1^{2-} from binding with the PVP block effectively.

Further addition of W_1^{2-} (to ∼300% ADN) caused almost no change in the zeta-potential from ∼0 mV, which did not turn to negative. This suggests that the interaction between W_1^{2-} and the PS-PVP-PEO micelle is mainly maintained by a charge interaction.

When PW_{11}^{7-} (Fig. 1b) or SiW_{11}^{8-} (Fig. 1c) was used as a counteranion, the zeta-potential of the micelle was steeply decreased to ∼0 mV at 100% ADN. This means that the affinity of POTs to the PVP block was high, and most of them were bound to the PS-PVP-PEO micelles. However, additional POTs (100∼800% ADN) caused further decrease in the zeta-potential, which turned to negative and finally settled down to −30∼−40 mV. Excess negative charge occurred in these complexes even after electrical neutralization was completed. This indicates that PS-PVP-PEO molecules bound PW_{11}^{7-} and SiW_{11}^{8-} by forces other than charge interaction. It is well known that POTs can bind PEO to form a quantitative (but not strictly stoichiometiric) complex, and this property has been applied to the quantification of nonionic detergents [34]. Although the detailed mechanism

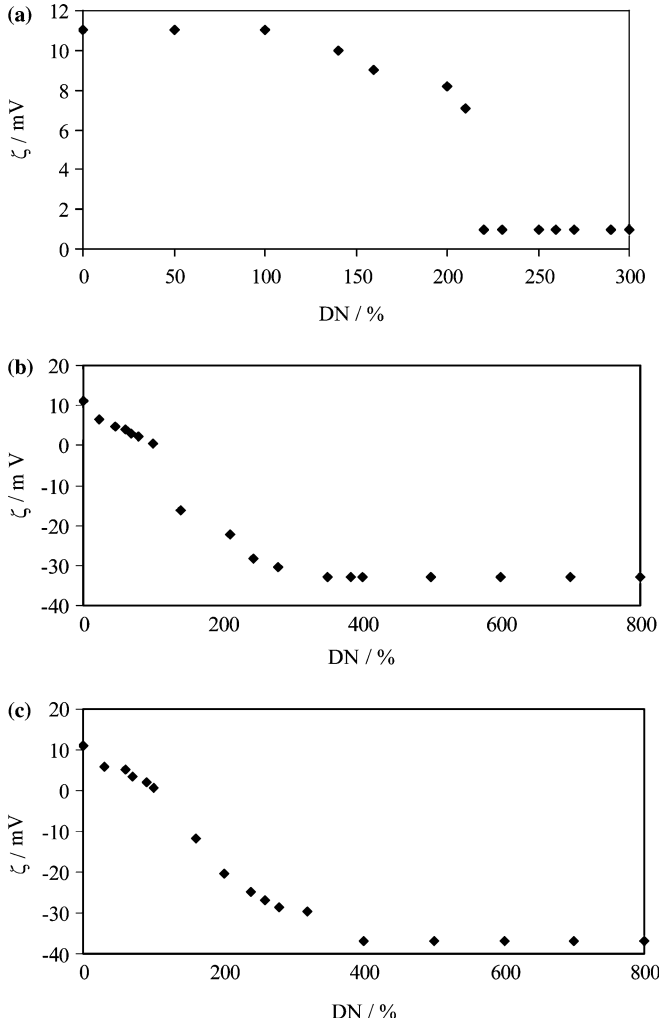

Fig. 1 Dose-dependency of counteranions in zeta-potential of PS-PVP-PEO micelle. Zeta-potential of PS-PVP-PEO micelles was measured at pH 3 with counteranions: **a** W_1^{2-}, **b** PW_{11}^{7-}, and **c** SiW_{11}^{8-} Concentration of PS-PVP-PEO was 0.025 g/L

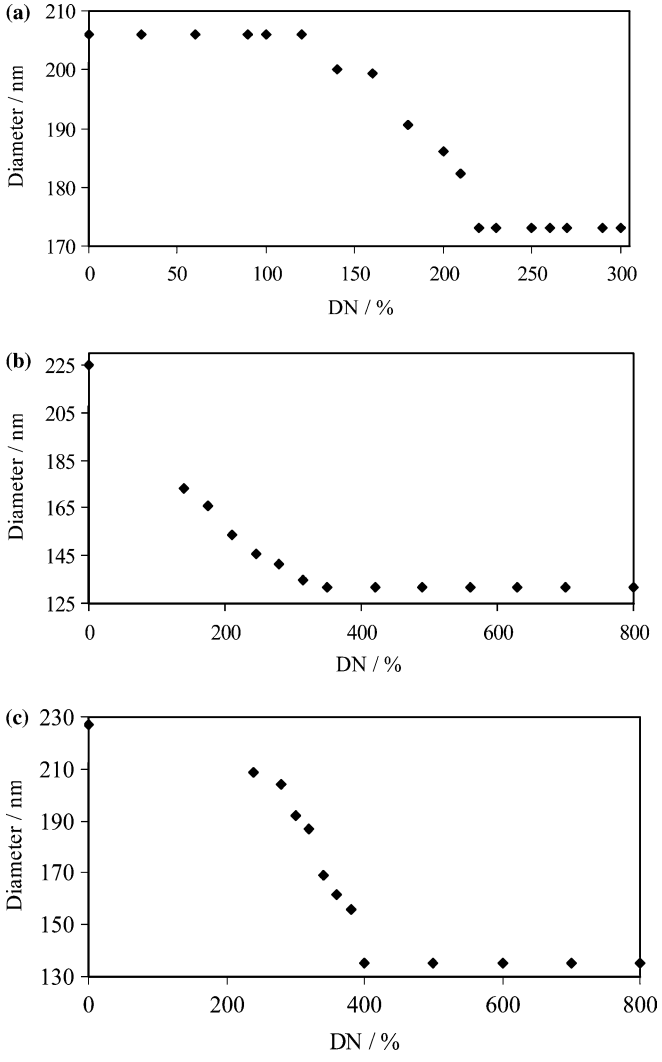

Fig. 2 Dose-dependency of counteranions in hydrodynamic diameter of PS-PVP-PEO micelles. Hydrodynamic diameter of PS-PVP-PEO micelles was measured at pH 3 with counteranions: **a** W_1^{2-}, **b** PW_{11}^{7-}, and **c** SiW_{11}^{8-} Concentration of PS-PVP-PEO was 0.025 g /L

of the interaction has not been elucidated yet, it is possible that: (1) The O-atoms in the PEO block were partially protonated to form oxonium cation, where POTs interacted by charge. (2) POTs polarized non-polar part of the PS-PVP-PEO molecule (e.g., the PEO block) with their very high negative charge and bound dipoles. (3) Hydrogen bonding occurred between the O-atoms in the POT molecule and H-atoms in the PS-PVP-PEO molecule. (4) The PS-PVP-PEO molecule formed an inclusion (clathrate) compound with POTs acting as a guest-like crown ether [35].

DLS measurements

In order to measure the change in hydrodynamic diameter of the PS-PVP-PEO micelles upon charge neutralization, the DLS of the micelles was measured. The results are shown in Fig. 2, and the hydrodynamic diameter (2 R_h) of the micelle was found to be around 200∼230 nm at pH 3 in the absence of a counteranion.

When W_1^{2-} was used as a counteranion (Fig. 2a), the hydrodynamic diameter of the micelle continuously decreased to ∼170 nm as ADN increased. This suggests that the micelle structure was shrunken due to the repulsive forces working among the PVP blocks were weakened by charge neutralization, as shown elsewhere [19, 21, 22]. However, the diameter did not minimize at 100% ADN, and an excess amount of W_1^{2-} (ADN = 220%) was required to do so. This means that the affinity for W_1^{2-} to the PS-PVP-PEO micelles was

relatively weak and/or steric hindrance occurred, as described in the former section.

When PW_{11}^{7-} (Fig. 2b) or SiW_{11}^{8-} (Fig. 2c) was used as a counteranion, the hydrodynamic diameter of the micelle became smaller (120∼130 nm) than that of the W_1^{2-}/PS-PVP-PEO complex. Although W_1^{2-} induced only ∼20% reduction in the micelle size at the most, PW_{11}^{7-} and SiW_{11}^{8-} gave ∼40% reduction. This means that charge neutralization of the micelles strongly occurred when the micelles were mixed with POTs. In addition, ADN giving the minimum hydrodynamic diameter on the micelles (350∼400%) was almost equivalent to that inducing the lowest zeta-potential on them (Fig. 1b, c). This suggests that morphological changes of the micelles were closely related to the charge.

It is noteworthy that the PS-PVP-PEO micelles still bound PW_{11}^{7-} and SiW_{11}^{8-} with continuously shrinking micelle size even after the zeta-potential turned to negative. This means that POT molecules were accumulated into the micelles against electrical repulsion. Although excess in positive charge maintained extended micelle conformation with a larger hydrodynamic diameter, overloading the negative charge by POTs rather caused further shrinking of the micelle size. This means that the negative charge induced by POTs did not work to separate PS-PVP-PEO molecules from each other, rather POTs grouped them to the center of the micelle like cross-linking glue. This is probably because PS-PVP-PEO molecules bound PW_{11}^{7-} and SiW_{11}^{8-} by forces other than charge interaction, as described in the former section.

The assay mixture inevitably contains a small amount of NaCl as a result of neutralization (pH adjustment) of HCl with NaOH. However, there was almost no effect on hydrodynamic diameters and zeta-potentials when 0.388 mM NaCl [equivalent NaCl concentration in PW_{11}^{7-} (or SiW_{11}^{8-})/PS-PVP-PEO complex solution at ADN = 800%] alone was mixed into in the PS-PVP-PEO micelle solution. Therefore, it was confirmed that the salt effect is negligible in the assay system.

Morphological studies

In the former two sections, it was suggested that the size of the PS-PVP-PEO micelles decreased when the positive charge in the PVP block was neutralized by POTs. In order to confirm this, the micelles were morphologically characterized with AFM (Fig. 3) and SEM (Fig. 4) techniques.

In AFM images, the average diameter of the PS-PVP-PEO micelle at pH 3 was 130 nm in the absence of the tungsten compounds (Fig. 3a). In the presence of PW_{11}^{7-}/SiW_{11}^{8-}, it was reduced to ∼80 nm at ADN = 350/400%, respectively (Fig. 3b, c). Although the micelle size was calculated to be smaller than the results of the DLS study, it was confirmed that POTs induced ∼40% reduction in the micelle size.

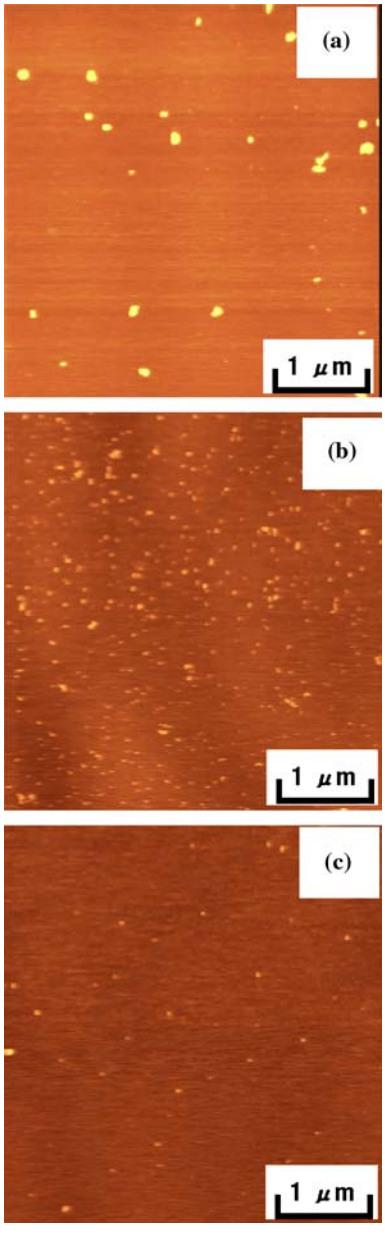

Fig. 3 Atomic force microscopic images of PS-PVP-PEO micelle. **a** PS-PVP-PEO alone, **b** PW_{11}^{7-}/PS-PVP-PEO complex at ADN = 350%, and **c** SiW_{11}^{8-}/PS-PVP-PEO complex at ADN = 400%

In SEM images, the mean size of the micelle was estimated as 110 nm in the absence of the tungsten compounds (Fig. 4a). In the presence of PW_{11}^{7-}/SiW_{11}^{8-}, the micelle size was reduced to ∼75 nm at ADN = 350/400%, respectively (Fig. 4b, c). In this case, the size reduction ratio induced by POTs was ∼35%.

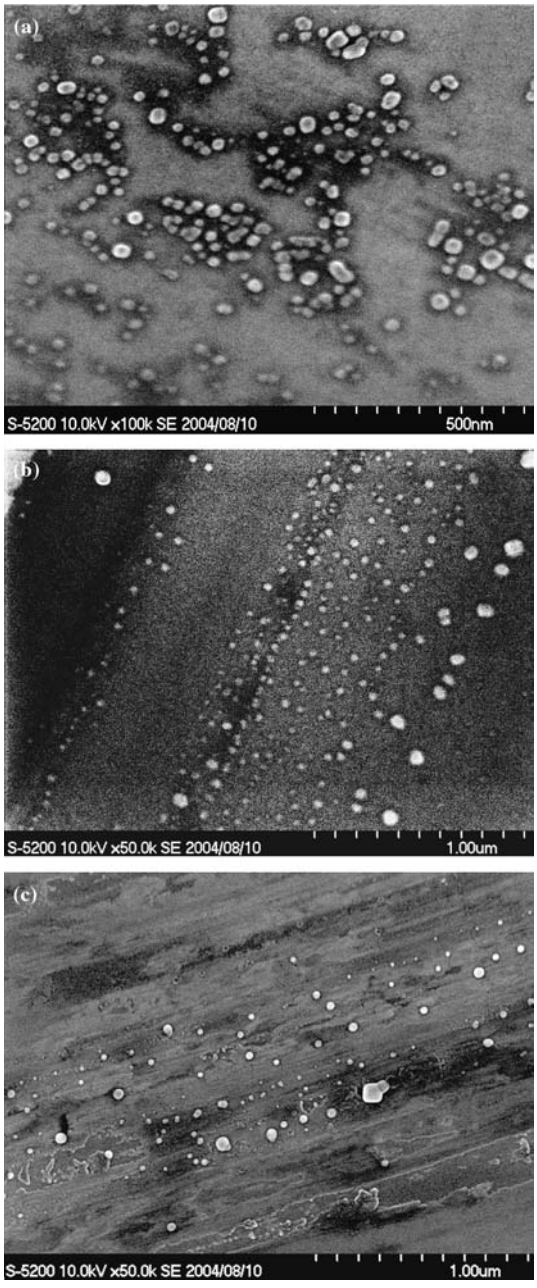

Fig. 4 Scanning electron microscopic images of PS-PVP-PEO micelle. **a** PS-PVP-PEO alone, **b** PW_{11}^{7-}/PS-PVP-PEO complex at ADN = 350%, and **c** SiW_{11}^{8-} /PS-PVP-PEO complex at ADN = 400%. Ten gradients correspond to 500 nm in (**a**), and to 1 μm in (**b**) and (**c**), respectively

It was observed that the morphology and size of the micelles were almost the same in both AFM and SEM studies. The size reduction ratio induced by POTs was in good accordance with the results of the DLS study. However, the hydrodynamic diameter given by the DLS study was larger than the size measured by AFM/SEM technique. This is probably due to the fact that AFM/SEM yields a number-averaged size whereas DLS does a *z*-averaged one. In addition, the hydration layers also count in DLS measurements.

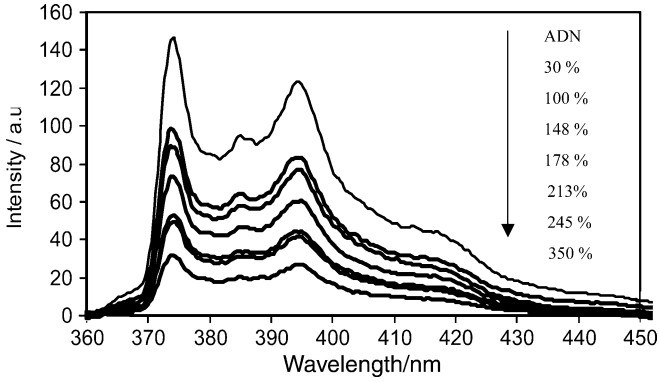

Fig. 5 Fluoresence spectra of Py in PS-PVP-PEO micelles. The fluorescence of Py (0.6 μM) with PW_{11}^{7-}/PS-PVP-PEO complex was measured in aqueous solutions (excitation = 334 nm). Concentration of PS-PVP-PEO was 0.025 g/L, and the amount of PW_{11}^{7-} expressed as ADN

Fluorescence spectroscopic study

Pyrene is a well-known fluorescent probe in which fluorescence intensity is easily affected by various kinds of molecular interaction with many factors [36, 37]. Therefore, the degree of molecular integration can be estimated from the signal intensity when Py is mixed with the micelle solution. Figure 5 shows fluorescence profile of 0.6 μM Py solution with PW_{11}^{7-} /PS-PVP-PEO nano-complex. As ADN was increased, the fluorescence intensity of Py decreased continuously and was finally minimized at ADN = 350%. Further addition of PW_{11}^{7-} caused almost no change, and excimer of Py was not formed judging from the pattern of fluorescent spectra.

The inner filtering effect of Py molecule is known to be relatively small, and Py is preferentially accommodated in polymeric micelles in aqueous solutions [38]. It was confirmed that a much higher concentration of PW_{11}^{7-} (in mM order) was required to induce the fluorescence quenching on Py molecules in the bulk phase of an aqueous solution (data not shown). Therefore, it was considered that the decrease in Py fluorescence shown in Fig. 5 is mainly attributable to the fluorescence quenching by interaction with PW_{11}^{7-} molecules accumulated in the core part of the micelles. In other words, it was confirmed that PW_{11}^{7-} is incorporated into the micelle of PS-PVP-PEO, forming an organic–inorganic nano-complex in aqueous solutions.

From the Stern–Volmer analysis (Fig. 6) on the fluorescence quenching of Py induced by PW_{11}^{7-}, a relatively higher Stern–Volmer constant ($K_{sv} = 1.45\times10^5$ M^{-1}) was

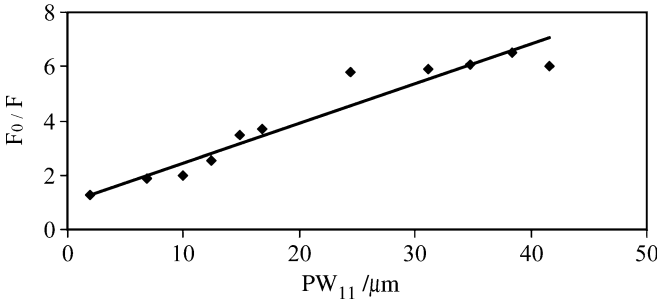

Fig. 6 Stern–Volmer plot for the quenching of Py flourescence in PW_{11}^{7-} /PS-PVP-PEO complex. The extent of fluorescence quenching of Py caused by PW_{11}^{7-} in aqueous solution was plotted

calculated (the inner filter effect caused by PW_{11}^{7-} was eliminated by a conventional method [39]). This means that both Py and PW_{11}^{7-} are highly concentrated into the PS-PVP-PEO micelles.

Conclusion

We succeeded in fabricating the organic–inorganic nano-complexes from tungsten compounds (W_1^{2-}, PW_{11}^{7-}, and SiW_{11}^{8-}) and PS-PVP-PEO triblock copolymer. The complexes were formed mainly by charge interaction between the cationic PVP block of the micelle and the counteranions. However, zeta-potential study and fluorescent analysis suggested that some other binding forces worked between PS-PVP-PEO micelles and POTs.

The addition of POTs into the PS-PVP-PEO micelles caused a significant morphological change in the micelles, and they became shrunken with ~40% size reduction ratio. This means that the structure of the micelles became tight, and the micelles could hold various materials tightly and thickly, as suggested by the high Stern–Volmer constant of a fluorescent probe. This feature may be useful to develop a new type of functioning micelle.

References

1. Fischer WR, Schwertmann U (1975) Clays Clay Miner 23:33
2. Sapiesko RS, Matijevic E (1980) J Colloid Interface Sci 74:405
3. Cornell RM (1985) Clays Clay Miner 33:219
4. Tadros ME, Mayes I (1979) J Colloid Interface Sci 72:245
5. Ishikawa T, Matijevic E (1991) Colloid Polym Sci 269:179
6. Ishikawa T, Matijevic E (1988) J Colloid Interface Sci 123:122
7. Kandori K, Horii I, Yasukawa A, Ishikawa T (1995) J Mater Sci 30:2145
8. Chittofrati A, Matijevic E (1990) Colloids Surf 48:65
9. Sakai H, Kawahara H, Shimazaki M, Abe M (1998) Langmuir 14:2208
10. Jana NR, Gearheart L, Murphy CJ (2001) Langmuir 17:6782
11. Pinna N, Weiss K, Sack-Kongehl H, Vogel W, Urban J, Pileni MP (2001) Langmuir 17:7982
12. Filankembo A, Andre P, Lisiecki I, Petit C, Gulik-Krzywicki T, Ninham BW, Pileni MP (2000) Colloids Surf A Physicochem Eng Aspects 174:221
13. Bronstein LM, Sidorov SN, Valetsky PM (1999) Langmuir 15:6256
14. Förster S, Antonietti M (1998) Adv Mater 10:195
15. Wegne G, Baum P, Müller M, Norwig J, Landfester K (2001) Macromol Symp 175:349
16. Cölfen H, Qi L (2001) Chem Eur J 7:106
17. Cölfen H (2001) Macromol Rapid Commun 22:219
18. Bronstein LM, Sidorov SN, Gourkova AY, Valetsky PM, Hartmann J, Breulmann M, Cölfen H, M Antonietti (1998) Inorg Chim Acta 280:348
19. Gohy JF, Willet N, Varshney S, Zhang JX, Jérôme R (2001) Angew Chem Int Ed 40:3214
20. Lei L, Gohy JF, Willet N, Varshney SK, Zhang JX, Jérôme R (2004) Macromolecules 37:1089
21. Khanal A, Li Y, Takisawa N, Kawasaki N, Oishi Y, Nakashima K (2004) Langmuir 20:4809
22. Gohy JF, Willet N, Varshney S, Zhang JX, Jérôme R (2002) e-Polymers No 35
23. Stepanek M, Humpolickova J, Prochakza K, Hof M, Tuzar Z, Spirkova M, Wolff T (2003) Collect Czech Chem Commun 68:121
24. Tajima Y (2005) Mini Rev Med Chem 5: in press
25. Li D, Guo Y, Hu C, Jiang C, Wang E (2004) J Mol Catal A Chem 207:183
26. Yang Y, Gao Y, Hun C, Wang E (2003) Appl Catal A Gen 252:305
27. Bragdon JH, Havel RJ (1954) Science 120:113
28. Tajima Y, Shizuka R, Oshitani S, Amagai H (1990) Thromb Res 57:697
29. Tajima Y (1997) J Inorg Biochem 68:93
30. Yamase T, Fukuda N, Tajima Y (1996) Biol Pharm Bull 19:459
31. Fukuda N, Yamase T, Tajima Y (1999) Biol Pharm Bull 22:463
32. Tajima Y (2001) Biol Pharm Bull 24:1079
33. Tajima Y (1999) J Biochem Biophys Methods 38:217
34. Shaffer CB, Dritchfield FH (1947) Anal Chem 19:32
35. Harris MJ (ed) (1992) Introduction to biotechnical and applications of poly(ethylene glycol). In: Biotechnical and biomedical applications, chap 1. Plenum, New York, p 4
36. Kalyanasundaram K, Thomas JK (1977) J Am Chem Soc 99:2039
37. Dong DC, Winnk MA (1982) Photochem Photobiol 35:17
38. Wilhelm M, Zhao C-L, Wang Y, Xu R, Winnik MA, Mura J-L, Riess G, Croucher MD (1991) Macromolecules 24:1033
39. Lakowicz JR (1983) Plenum Press, New York